Supporting Information

Mesoscale Anatomy of Dead Lithium Formation

Deepti Tewari,[1] Sobana P. Rangarajan,[1] Perla B. Balbuena,[2] Yevgen Barsukov,[3] and Partha P. Mukherjee[1,*]

[1]School of Mechanical Engineering, Purdue University, West Lafayette, IN 47907, USA

[2]Department of Chemical Engineering, Texas A&M University, College Station, TX 77843, USA

[3]Texas Instruments, Dallas, TX 75243, USA

*Correspondence: pmukherjee@purdue.edu (Partha P. Mukherjee)

Transition events in Kinetic Monte Carlo Algorithm

The KMC model includes three processes, the diffusion of lithium ions in the electrolyte, the electrochemical oxidation of lithium at the electrode-electrolyte interface and diffusion of lithium at solid electrode interface. A rejection free and partial search KMC algorithm is used [1–3]. A detailed description of the algorithm is given in [4].

The value of the parameters used in describing the three rates given by equation 2, 3 and 4 is listed in Table S1. The local overpotential and temperature values are typical of battery operations. The range for ionic diffusion barrier is based on different molecular dynamics studies for different electrolyte composition. The activation energy for surface diffusion of lithium on (100) plane is 0.14 eV and 0.41 eV on (111) plane for hopping mechanism [5]. In the two dimensional KMC model, surface diffusion barrier values ranging from 0.14 eV to 0.25 eV is used to study the effect of surface diffusion on the process of formation of dead lithium. This range of surface diffusion barriers is sufficient to show that surface diffusion is one of the key factors in formation of dead lithium.

Table S1: Parameters used in KMC model

Symbol	Description	Value	Units
η	Overpotential	0.01 to 0.125	Volts
T	Temperature	-25 to 50	^{o}C
j_0	Exchange current density	2 [6]	mA/cm^2
α_a	Anode charge transfer coefficient	0.3 [6,7]	
α_c	Cathode charge transfer coefficient	0.7 [6,7]	
a	Lattice constant for lithium	3.5×10^{-10}	m
ΔE_e	Activation energy barrier for diffusion of lithium ion in the electrolyte	0.1 to 0.2 [8–11]	eV
ΔE_s	Activation energy barrier for diffusion of lithium atom on solid surface of the interface	0.14 to 0.25 [5]	eV

Calculation of Surface Ratio

The surface ratio is used to characterize the average nature of the interface [4]. Figure S1 describes the procedure to calculate the surface ratio. If N1 is the number of lattice points on the envelope of the interface and N is the number of lattice points on the actual interface, then the surface ratio is defined as the ratio of N and N1. If the surface ratio is less than one, the interface is convex, if it is equal to one, the interface is flat, if it is greater than one, the interface is concave.

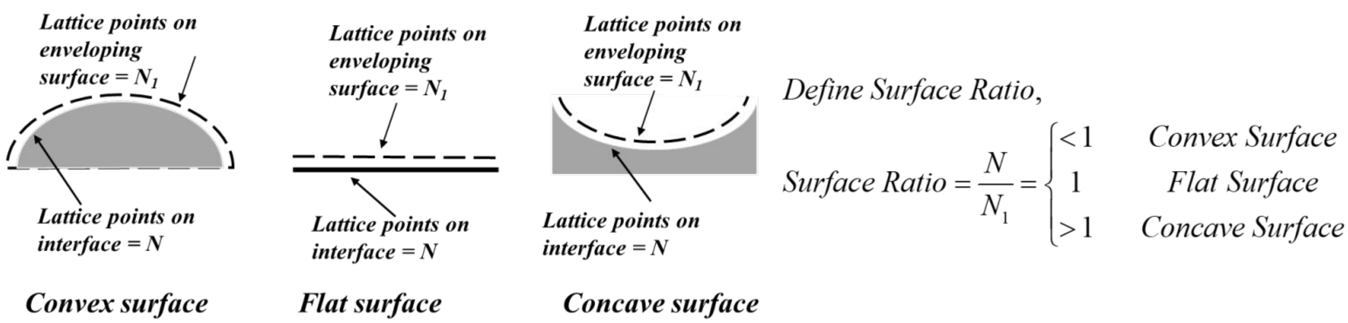

Figure S1: Schematic describing how to calculate the surface ratio.

Computational Domain

In the two dimensional lattice based KMC model, N_x is the number of lattice points in the horizontal direction and N_y is the lattice points in the vertical direction. Initially, 50 layers are lithium, ($0 \leq N_y \leq 50$) is lithium electrode and the rest is lithium ions distributed in electrolyte. The computational domain is periodic in horizontal direction. To study the effect of domain size, the number of lattice points in the horizontal direction is increased from 25 to 200 while the number of layers of lithium and the lattice points in the vertical direction is kept constant. In Figure S2(a), the number of dissolved layers is plotted with increasing N_x and in (b), the number of layers of dead lithium is plotted with increasing N_x. It can be seen that there is not strong dependence on the size of the computational domain. Based on the plots shown in (a) and (b), N_x=150 has been used in all KMC simulations.

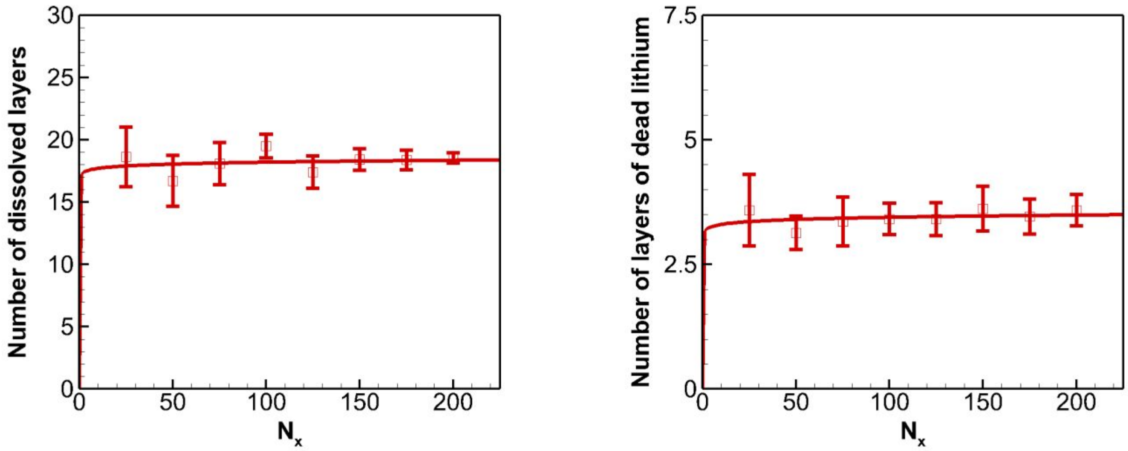

(a)	(b)

Figure S2: Domain size during stripping of lithium electrode. (a) Number of dissolved layers with increasing domain size N_x (b) Number of layers of dead lithium with increasing N_x. These studies were performed using overpotential of 0.01 V and temperature of 25 ^oC.

Experimental Details

All materials were handled in an Argon-filled glovebox (MBraun), with water and moisture levels below 0.5 ppm. A typical electrolyte with 1 M LiPF6 in 1:1 (volume ratio) ethylene carbonate/ethyl methyl carbonate (EC/EMC) (BASF) and lithium chips of 14 mm diameter and 0.75 mm thick (MTI) were used in this work. Celgard 2500 polypropylene separators were used in between two lithium electrodes. All the electrodes were assembled in CR2032 type coincells. The stripped electrodes were harvested from the cells after discharge at 1 mA/cm2 and 2 mA/cm2. The stripped lithium metal electrode was examined and imaged under a Leica S9i Microscope. For each current density, three identical cells were assembled and cycled at three different temperatures, i.e. at -20^oC, 20 ^oC and 40 ^oC respectively.

Image analysis

The amount of dead lithium is quantified based on the pixel intensity values. As the color of the lithium varies with passivation with electrolyte as well as the texture, we used a histogram based method to identify the threshold value instead of setting a manual threshold.

In addition to this, the imaging conditions may affect the outcomes significantly. In order to avoid this, all imaging conditions such as the sample orientation, working distance and the level of light were same for all the electrode images.

Image color thresholding was used to select the dead lithium particles by choosing a specific pixel color value as the threshold. The dead lithium particles exhibit particular range of pixel color values. The range is identified by calculating the mode from the histograms of dead lithium crystals. Figure S3 shows the different thresholding algorithms applied for segmentation of the image. We use minimum method for threshold as it effectively helps us avoid errors caused by continuous structures such as ridges, pits in the electrode as well as the occasional dullness of the surface caused by the passivation of lithium with electrolyte from the dead lithium particles shown in the highlighted box in Figure S3.

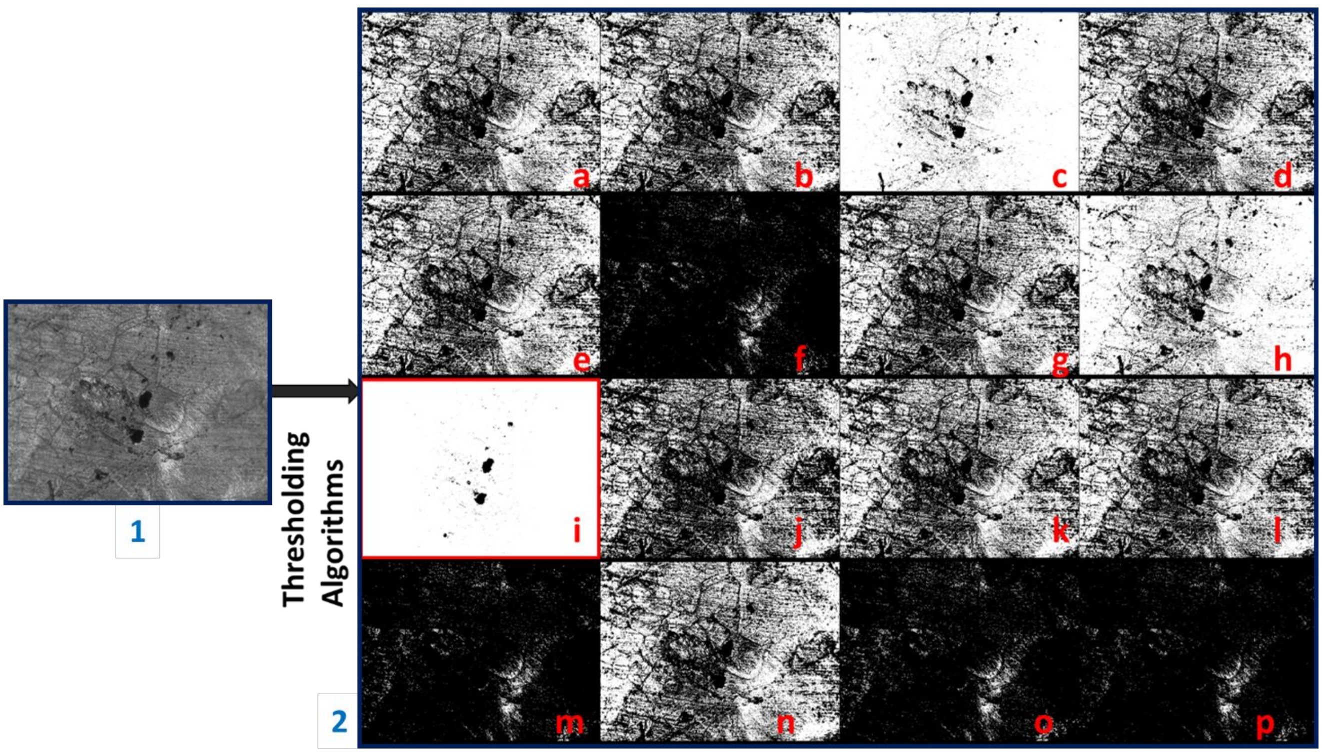

Figure S3: (1) Original image of stripped electrode; (2) Binary Image after applying different thresholding algorithms on original image shown in (1) (a) Default Algorithm (b) Huang Algorithm (c) Intermodes Algorithm (d) IsoData Algorithm (e) Li Algorithm (f) MaxEntropy Algorithm (g) Mean Algorithm (h) MinError(I) Algorithm (i) Minimum Algorithm (j) Moments Algorithm (k) Otsu Algorithm (l) Percentile Algorithm (m) RenyEntropy Algorithm (n) Shanbhag Algorithm (o) Triangle Algorithm (p)Yen Algorithm. The minimum algorithm shown in (i) shows the binary image where the threshold is not affected by the surface roughness factor or dullness.

Once the threshold is set, the pixels with values greater than the threshold value will be discounted as the background. Only the pixels with values less than or equal to the threshold will remain. In our case, these pixels represent dead lithium particles. The image is binarized after thresholding process for particle analysis. The black regions indicate dead lithium particles. The area of each particle is calculated by the product of the estimated number of pixels in the particle and area of a pixel. Figure S4 (a), (b) and (c) illustrate the flowchart of image analysis for dead lithium quantification.

In order to map the surface morphology of the stripped electrode, a luminescence based surface plot is obtained using the hue, brightness and saturation of each pixel in the image. Based on the surface topography, the amount of light reflected by the surface varies. The pixel values range from 0-255, where zero represents black and 255 represents white. Point tips reflect specular light and hence appear white with pixel values around 255. Pits absorbs and diffracts light and hence appear dark, closer to pixel values around zero. Based on this, the surface of the electrode is reconstructed as shown in Figure S4 (d) and (e).

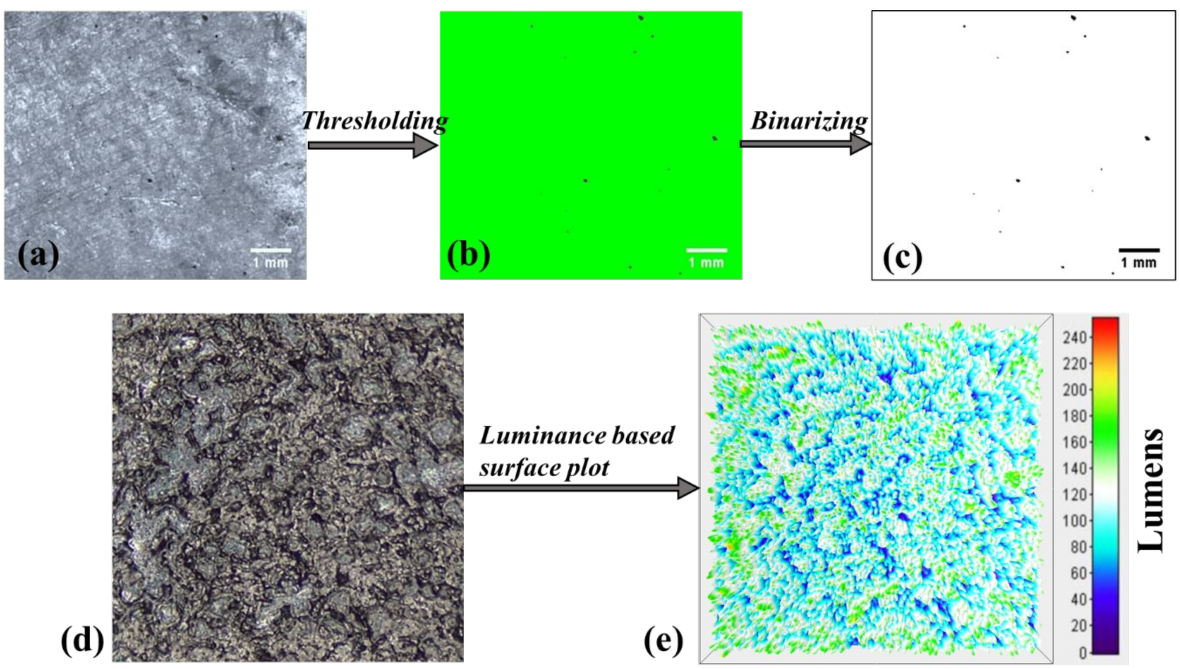

Figure S4: (a) Original image of stripped electrode; (b) Image after thresholding based on pixel values, black particles represent the pixels with values less than the threshold, the green part represents the pixel values above the threshold; (c) Binarization of thresholded image, black particles represent dead lithium crystals; (d) Image of stripped electrode with intense pitting of size 530×530 μm (200×200 pixels); and (e) Image reconstructed as surface plot based on the luminescence values of pixels.

The voltage and current profile of the Li-Li symmetric cells at different temperatures during the three-hour discharge is shown in Figure S5(a) and (b) at 1mA/cm^2 and 2 mA/cm^2.

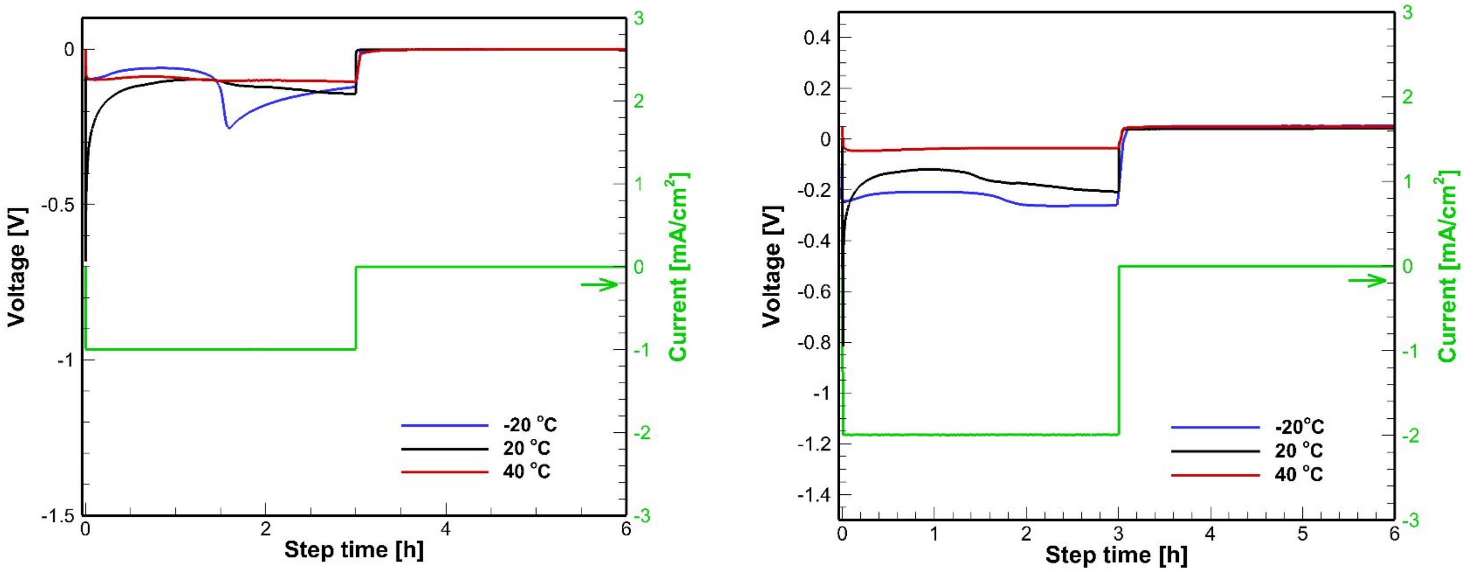

(a) (b)

Figure S5: Voltage profile of a Li-Li symmetric cell cycled (a) at 1 mA cm^2, (b) at 2 mA/cm^2

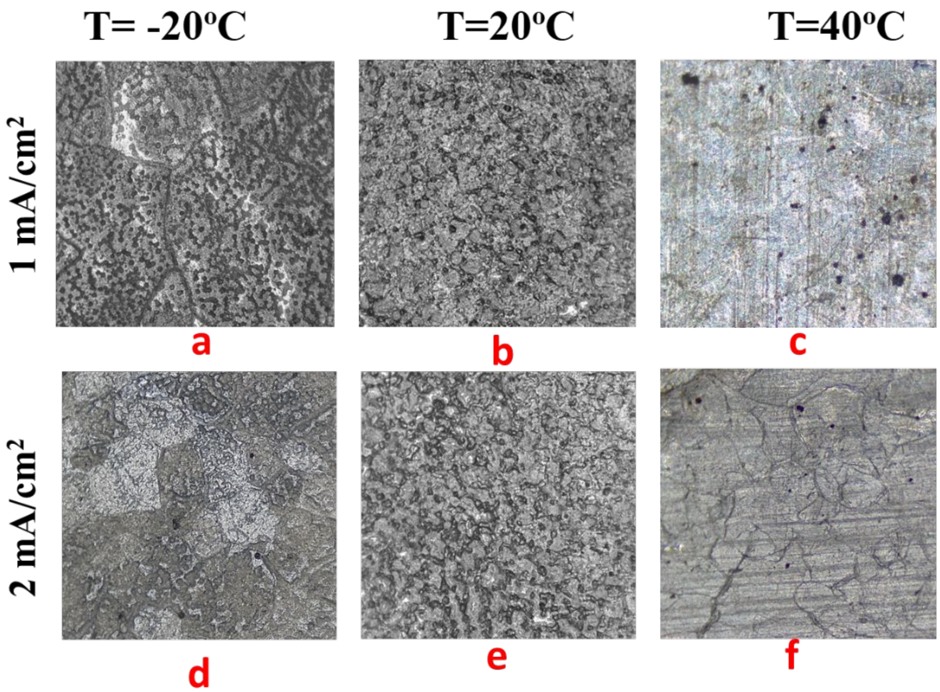

Figure S6: Original images of stripped lithium electrode (top view): at current density 1 mA/cm^2 at (a) -20^o C, (b) 20^o C, (c) 40^o C, and at current density 2 mA/cm^2 at (d) -20^o C, (e) 20^o C, (f) 40^o C.

References

(1) Schulze, T. P. Efficient Kinetic Monte Carlo Simulation. *J. Comput. Phys.* **2008**, *227* (4), 2455–2462.

(2) Turner, C. H.; Zhang, Z.; Gelb, L. D.; Dunlap, B. I. Kinetic Monte Carlo Simulation of Electrochemical Systems. *Rev. Comput. Chem.* **2015** (*28), 175-204*.

(3) Voter, A. F. Introduction To the Kinetic Monte Carlo Method. In *Radiation Effects in Solids*; 2011; pp 1–23.

(4) Tewari, D.; Mukherjee, P. P. Mechanistic Understanding of Electrochemical Plating and Stripping of Metal Electrodes. *J. Mater. Chem. A* **2019**, *7*, 4668–4688.

(5) Jäckle, M.; Groß, A. Microscopic Properties of Lithium, Sodium, and Magnesium Battery Anode Materials Related to Possible Dendrite Growth. *J. Chem. Phys.* **2014**, *141* (17), 174710.

(6) Arora, P.; Doyle, M.; White, R. E. Mathematical Modeling of the Lithium Deposition Overcharge Reaction in Lithium-Ion Batteries Using Carbon-Based Negative Electrodes. *J. Electrochem. Soc.* **1999**, *146* (10), 3543–3553.

(7) Ge, H.; Aoki, T.; Ikeda, N.; Suga, S.; Isobe, T.; Li, Z.; Tabuchi, Y.; Zhang, J. Investigating Lithium Plating in Lithium-Ion Batteries at Low Temperatures Using Electrochemical Model with NMR Assisted Parameterization. *J. Electrochem. Soc.* **2017**, *164* (6), A1050–A1060.

(8) Bhatt, M. D.; Cho, M.; Cho, K. Density Functional Theory Calculations and Ab Initio Molecular Dynamics Simulations for Diffusion of Li^+ within Liquid Ethylene Carbonate. *Model. Simul. Mater. Sci. Eng.* **2012**, *20*, 065004.

(9) Borodin, O.; Smith, G. D. Quantum Chemistry and Molecular Dynamics Simulation Study of Dimethyl Carbonate: Ethylene Carbonate Electrolytes Doped with $LiPF_6$. *J. Phys. Chem. B* **2009**, *113* (6), 1763–1776.

(10) Soetens, J.-C.; Millot, C.; Maigret, B. Molecular Dynamics Simulation of $Li^+BF_4^-$ in Ethylene Carbonate, Propylene Carbonate, and Dimethyl Carbonate Solvents. *J. Phys. Chem. A* **1998**, *102* (7), 1055–1061.

(11) Ong, M. T.; Verners, O.; Draeger, E. W.; Van Duin, A. C. T.; Lordi, V.; Pask, J. E. Lithium Ion Solvation and Diffusion in Bulk Organic Electrolytes from First-Principles and Classical Reactive Molecular Dynamics. *J. Phys. Chem. B* **2015**, *119* (4), 1535–1545.